Mini review

Recent Progress in Electrochemical Detection of C-Reactive Protein: A Review

Changdong Chen, Ming La, Kesheng Cao and Guoping Cheng*

College of Chemistry and Chemical Engineering, Pingdingshan University, Pingdingshan, Henan 467000, People's Republic of China
*E-mail: mingla2011@163.com

Numerous studies have revealed that C-reactive protein (CRP) is high related to some diseases such as inflammation and cardiovascular. Thus, CRP has been considered as a predominant protein biomarker. Urgent requirement in assay of CRP has dramatically accelerated the emergence of high-performance detection technologies. This review summarizes the advances in development of electrochemical biosensors for CRP detection based on various sensing methodologies and strategies.

1. INTRODUCTION

CRP (α-globulin of 120 kDa), an acute phase reactant, is quickly produced by the liver once a biological organism suffers inflammation, invasion of microorganisms or tissue damage. CRP has been considered as a highly sensitive biomarker for inflammation, infection and cardiovascular disease risk [1]. The routine and accurate CRP quantification is of great importance to identify the state of disease and judge the efficacy of treatment intervention. Normally, the concentration of plasma CRP is below 1.0 mg/L, and the clinical diagnostic level ranges from 1 to 3 mg/L in healthy humans. According to the classification of the CRP levels for evaluating the cardiovascular disease risk by The American Heart Association and the United States Centre for Disease Control, it is a low risk below 1.0 mg/L, an average risk within 1.0 – 3.0 mg/L, a high risk above 3.0 mg/L [2]. Thus, sensitive and selective methods for the measurement of CRP concentration is extremely significant for effective disease diagnose and early intervention.

In clinical laboratories, several original methods have been successfully applied for CRP detection, including immunoturbidimetry [3,4], immunoagglutination [5] and the enzyme-linked

immunosorbent assay (ELISA) [6-8]. Although these methods are well-established and reliable, these methods always suffer from severe disadvantages such as high-cost, time-consuming, low sensitivity, dependence of skillful operation and expensive instruments [9]. In the past few decades, with the development of instrumental methods and nanotechnologies, various powerful methods have been proposed for the rapid and accurate detection of CRP, such as surface plasmon resonance (SPR) spectroscopy [10,11], colorimetry [12-14], surface-enhanced raman spectroscopy [15,16], fluorescence spectroscopy [17-19], chemiluminescence spectroscopy [20], electrochemiluminescence spectroscopy [21,22] and photoelectrochemical methods [23,24].

Among these reported methods, electrochemical biosensors are of particular interest for biochemical analysis, because of the advantages of low-price, rapid response, high sensitivity, good selectivity, wide dynamic concentration response range and small sample volume [25,26]. In recent years, different electrochemical technique, such as voltammetry and amperometry, have received extensively research interest and have been widely utilized in the detection of various disease markers [27-29]. This review focuses on the recent development of electrochemical methods for CRP detection. Moreover, we attempted to put a particular emphasis on electrochemical methodologies based on nanomaterials (NMs) with plenty of characteristic properties.

2. LABEL-FREE METHODS

The cost, time consuming, and nonspecific signal along with modification have push scientists to develop label-free assays. Electrochemical analytical methods as a main class of interfacial techniques, have been widely used, based on recording impedance, current, potential, and conductivity signals. Among those label-free electrochemical assays, electrochemical impedance spectroscopy (EIS) and electrochemical capacitative spectroscopy (ECS) have attracted extensive attention in the development of electrochemical sensors and the nondestructive characterization of electrode surface, since it can sensitively detect the substantial perturbation in capacitance or charge-transfer resistance associated with material binding or modification on the electrode surface [30]. Among various electrodes used in label-free electrochemical biosensors, the screen-printing electrode (SPE) has been mass produced and used because it is a disposable, combustible and low-cost substrate. The integration of the label-free detection strategy into SPE-based electrochemical biosensors has received more interest in various applications. Capture probes for recognition of CRP include antibodies, phosphocholines, or aptamers, by which this section was classified.

2.1 Antibody as the receptor

Immunoglobulin antibodies, including polyclonal and monoclonal antibodies, are high molecular weight proteins produced from immune cells, which could bind to specific protein ''foreign objects'' (targets) [31]. Up to now, many thousands antibodies are commercially available worldwide. Antibodies composed of amino acid residues, containing nitrogen and/or sulfur atoms, could be covalently bound on gold-based electrodes [32-34]. For example, Brito-Madurro's group directly immobilized anti-CRP antibody onto a gold-printed screen electrode (Au-SPE) via the stable high-

affinity thiolate-gold bonds (40-50 kcal/mol) [35]. Along with the formation of sandwich-type immune-complex, the faradaic reaction is highly hindered, resulting in an increase in the charge transfer resistance (R_{ct}) and an obvious decrease in the anodic current. Omanovic's group investigated the performance of different electrochemical techniques to probe the interaction between CRP and antibody, in following decreasing order of the sensitivity: DPV, EIS, CV and ECS [36]. Ramakrishna's group overlaid a biogenic nanoporous silica membrane on top of an array of gold electrodes to form a high density of nanowells [37]. As illustrated in Figure 1, Zhu's group reported an EIS immunosensor for CRP based on three-dimensionally ordered macroporous (3DOM) gold film [38]. The 3DOM gold film composed of interconnected gold nanoparticles was electrochemically fabricated with an inverted opal template, the surface area of which was 14.4 times higher than that of a classical bare flat one. Thanks to the good biocompatible microenvironment and the increase of conductivity and stability provided by the 3DOM gold film, the proposed immunosensor exhibited a linear concentration range of 0.1 to 20 ng mL^{-1} and a limit of detection (LOD) of 0.1 ng mL^{-1}. Han's group prepared a highly specific immunosensor chip using a gold (Au) wire/polycarbonate substrate to detect CRP with a detection limit of 2.25 fg/mL [39]. Cho's group developed an ECS immunosensor for CRP by modify interdigitated wave-shaped micro electrode array (IDWµE) with a self-assembled monolayer of dithiobis (succinimidyl propionate) (DTSP) [40]. Well-defined SAMs of novel (R)-diaza-18-crown-6 and 3-cyanopropyltrimethoxysilane (3-CPTMS) on gold and ITO electrodes were also used for label-free detection of antibody-CRP interactions [41,42].
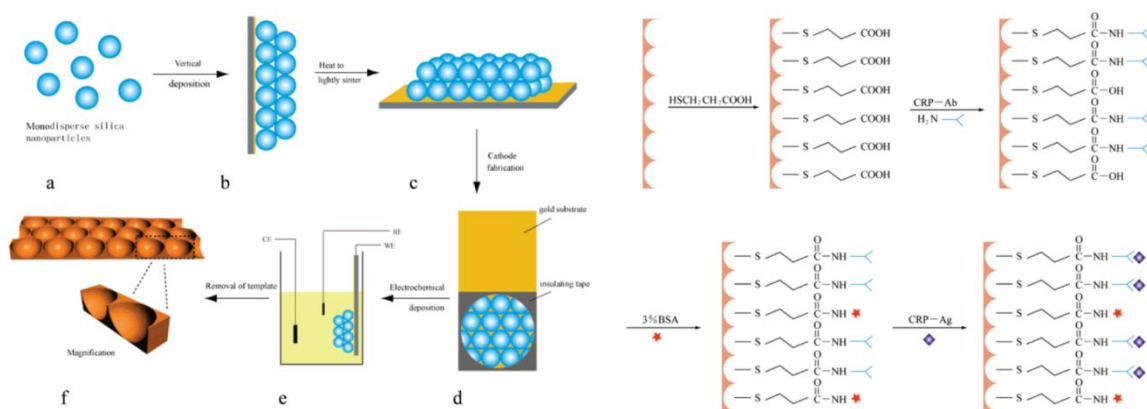

Figure 1. Schematic of the procedure for preparation of 3DOM gold film electrodes (left) and the stepwise immunosensor fabrication process (right). Reprinted with permission from reference [38]. Copyright 2008 American Chemical Society.

In recent years, ECS based on pure dielectric and redox active molecular films have attracted numerous attention, in which the redox capacitance (C_r) of the surface confined electroactive film is very sensitive towards its electrostatic environment. Bueno's group fabricated a mixed SAM of pentadecanethiol and 11-ferrocenyl-undecanethiol (11-FcC) and further modified with anti-CRP antibodies for ECS detection of CRP [43]. The CRP binding induced a progressive perturbation in film faradaic activity sensitively probed by capacitance. As shown in Figure 2, they prepared mixed alkylferrocene−poly(ethylene glycol) (PEG)−antibody films for CRP with a LOD of 28 pM [44].

Recently, they further modified the SAM of 11-FcC with graphene oxide (GO) and CBMA zwitterionic monomer [2-carboxyN,Ndimethyl-N-(2'-methacryloyloxyethyl) ethanaminium inner salt], endowing specific CRP bio-recognition interface with non-fouling characteristics [45]. A SAM of a ferrocene redox tagged peptide on gold electrode was also used for ECS detection of CRP [46].
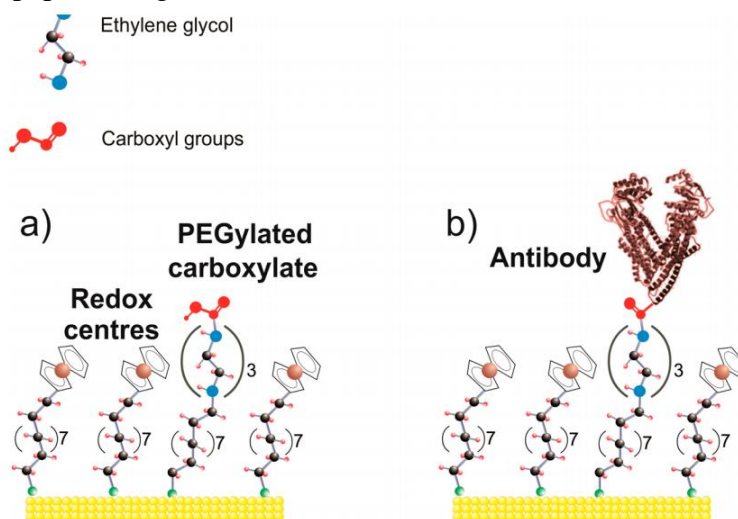

Figure 2. Schematic of the preparation of mixed PEG-anchored antibody and thiolated ferrocene films. Reprinted with permission from reference [44]. Copyright 2014 American Chemical Society.

Due to their distinguish electrochemical properties, π-π-conjugated intrinsically electrically conducting polymers such as polypyrrole (PPy), polythiophene and polyaniline (PANI) have been extensively investigated in electrochemical sensors/biosensors application. Brito-Madurro's group fabricated nanostructured poly(3-aminothiophenol) (PATP) films for the detection of CRP [47]. Davis' group proposed an electrochemical biosensor for reagentless redox capacitive assaying of CRP based on phytic acid-doped polyaniline (PANI-PA) films (Figure 3) [48]. In this report, the redox film were generated via electropolymerization as a novel redox-charging polymer support, in which phytic acid doping endow the polymeric films with higher conductivity and high hydrophilicity. The surface coverage and redox properties of generated films could be facilely tuned, affecting the selectivity, fouling, and sensitivity of the assay. The optimal balance of sensitivity and fouling was achieved at PANI-10 min, and the CRP sensor showed a linear range of 0.25−2 μg/mL with a LOD of 0.5 μg/mL. It has been reported that the electroconductivity of polymers can be further improved by incorporating with ions, metals, or metal oxides NMs. Moreover, NMs integrated into polymer film may be an efficient substrate for the immobilization of biomolecules without degrading their bioactivities. Rajesh's group electrochemically intercalated 3-mercaptopropionic acid (MPA)-capped Pt and Au NPs in the PPy matrix using a one-step electrochemical method for CRP detection [49,50]. Molybdenum disulfide–polyaniline–gold nanoparticles (MoS$_2$–PANI–GNPs) with high conductivity were synthesized as the substrate to accelerate the electron transfer for CRP determination [51].
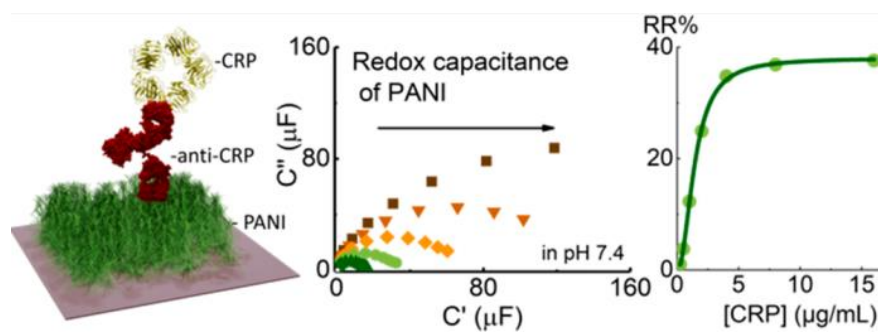
Figure 3. Schematic of reagentless redox capacitive assaying of CRP at a polyaniline interface. Reprinted with permission from reference [48]. Copyright 2020 American Chemical Society.
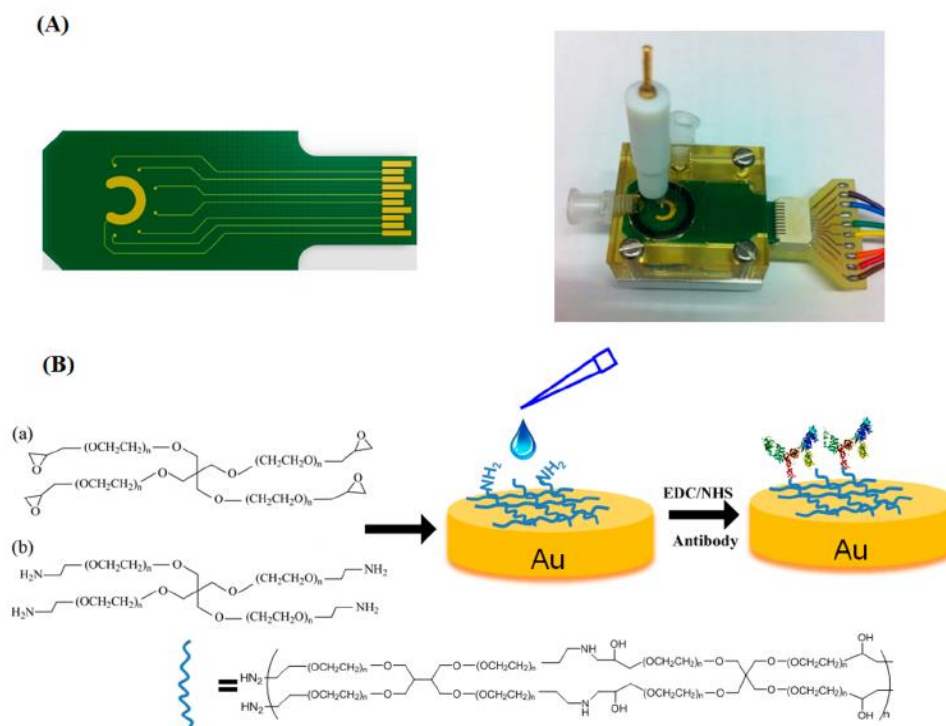

Figure 4. (A) Utilized microfabricated arrays (left) and their associated fluidic housing (right). (B) Schematic representation of the cross-linked functional PEG polymer electrode modification and subsequent antibody integration. Reprinted with permission from reference [52]. Copyright 2014 American Chemical Society.

Nowicka's group electropolymerized branched polyethylenimine functionalized with ferrocene residues (PEI-Fc) on the electrode surface for covalently binding more anti-CRP antibodies and providing voltammetric detection signal [53]. Due to their large surface areas and plenty of functional groups, poly(amidoamine) (PAMAM) dendrimers are frequently used for immobilizing biorecognition probes for biosensor design. Karaboğa's group used 11-cyanoundecyltrimethoxysilane (CUTMS) and PAMAM dendrimers (G:1 amino surfaces) to modify indium tin oxide (ITO) disposable electrodes and further immobilize the anti-CRP antibody via covalent interactions [54]. Despite the relative simplicity, during applications in real samples detection, label-free electrochemical biosensors often encounter the poor signal-to-noise ratio and high background signal. Various biofoulants (proteins,

cells, polysaccharides and lipids) contained in clinical complex solutions are prone to attach to the electrode surface through nonspecific binding, resulting in an obstruction for electron diffusion. Therefore, it is necessary to design an antifouling sensing platform for effectively reducing undesired binding on the electrode surface to maintain biosensor performance in practical analysis. Among plenty of antifouling materials integrated on the electrode surface, poly(ethylene glycol) (PEG) polymer are extensively used due to well biocompatibility, naturally inert and hydrophilicity. Davis' group integrated cross-linked PEG polymer films generated from commercial PEGylated monomers within fabricated microelectrode arrays for simultaneous detection of insulin and CRP in human serum (Figure 4) [52]. An optimized molar ratio (2:3) of 4-armed PEG-epoxide and PEG-amine was selected for the formation of the thermo-polymerized film, ensuring enough accessible amine groups for antibody attachment and the performance of the resulting biosensor. In the absence of amplifying redox probes, CRP was monitored by non-Faradaic EIS with a linear range of 0.5 ~ 50 nM (R^2 = 0.997) and a LOD of 150 ± 10 pM.

Cellulose nanofibril not only is biocompatible and biodegradable, but also has unique nanostructures in films with high mechanical strength, small porosity and high density. Rojas' group reported an immunosensor for CRP detection based on carboxylated nanofibrillar cellulose (NFCs) by quartz crystal microgravimetry (QCM) [55]. As displayed in Figure 5, they designed two ways to achieve ultrathin films of carboxylated NFCs, including carboxymethylation after/before immobilization of NFCs on the electrode. Protein A was selected as a ligand for the oriented immobilization of anti-CRP to improve the sensitivity and selectivity of immunosensors. Under the optimal conditions, CRP in the range of 1 to 100 μg/mL could be sensitively detected. Moreover, this NFCs-based immunosensor showed excellent nonspecific protein resistance against biomolecules.
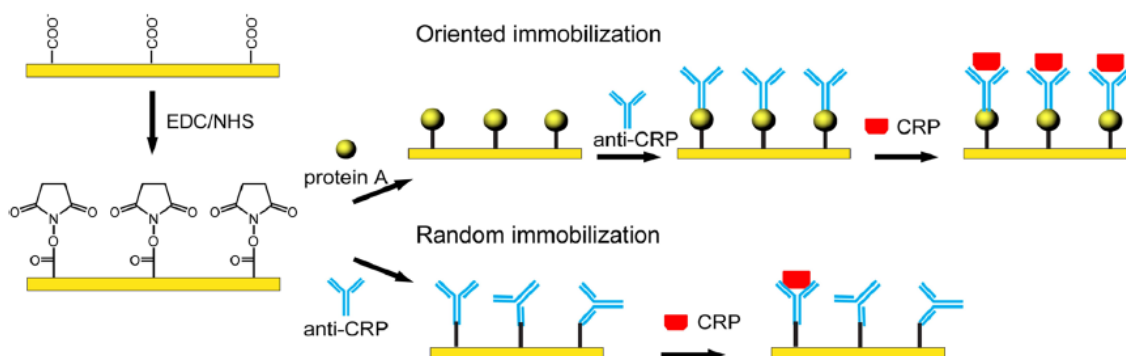

Figure 5. Immobilization of Anti-CRP on carboxylated CNF surfaces (tCNF or cCNF) via EDC/NHS coupling for CRP detection. Reprinted with permission from reference [55]. Copyright 2016 American Chemical Society.

Owing to the attractive advantages of a high surface area to immobilize more antibodies, high electrical conductivity, well chemical stability and excellent biocompatibility, NMs have been broadly employed to modify the electrode for enhancing the sensitivity and selectivity. Carbon nanotubes (CNTs), including multiwalled CNTs (MNCNTs) and singlewalled CNTs (SNCNTs) have been often employed for fixing antigen/antibody molecules to prepare biomolecules-modified electrodes with

high sensitivity. Yang's group synthesized bioactive multiple-bent MNCNTs on a carbon film (CF) layer (MWCNTs/CF) for electrochemical immunosensing of CRP at low concentrations [56]. Moreover, to endow more functionality into CNTs and improve the performance of resulted biosensors, scientists have used different materials to decorate CNTs. For example, Cao's group prepared Fe_3O_4 (core)/Au (shell) NPs-coated multiwalled carbon nanotubes (MWCNT–GMP) for immobilizing anti-CRP and further adsorbed the hybrids on the surface of N,N"-bis-(2-hydroxy-methylene)-o-phenylenediamine cobalt (CoRb) modified SPEs through external magnetic field [57]. Since Geim's group first isolated single-layer graphene from graphite in 2004, extensive focuses have been put into graphene and its derivates in various research fields. Chailapakuls's group fabricated graphene-modified SPE (G/SPCE) using an in-house screen-printing method on an origami paper and subsequently modified G/SPCE with electrodeposited AuNPs and L-cysteine for capture anti-CRP immobilization and CPR measurement [58]. Pt NPs-graphene modified glassy carbon electrode (GCE) and Au NPs-reduced graphene oxide (rGO)-modified indium tin oxide (ITO) microdisk electrode array (MDEA) chips were also used to quantitively detect CRP by EIS [59,60]. Graphene quantum dots (GQDs), as an emerging type of graphene, have aroused a increased interest in recent years for their interesting optical, electronic, and biochemical properties. Bing's group applied GQDs produced from hydrothermal cutting graphene to develop an label-free electrochemical immunosensor for CRP detection [61]. Vertically aligned carbon nanofibers (VACNFs) formed by plasma enhanced chemical vapor deposition can improve the roughness of the electrode surface and confirm the orientation of the antibody, which is one type of individual free-standing nanostructures suitable for nanoelectrode arrays (NEA) construction [62]. For instance, Koehne's developed VACNFs-based electrochemical biosensors for label-free detection of CRP [63,64]. Diamond, an allotrope of graphite, has been proved as a novel transducer material for biosensor development due to its excellent physical, chemical and electrical characteristics. Michiels' group applied the hydrogen (H)-terminated surface of nanocrystalline diamond (NCD) to physically adsorb anti-CRP antibodies for impedimetric detection of CRP [65].

Au NPs was utilized to modify the cysteamine-assembled gold electrode to provide an active substrate for the immobilization of CRP antibody [66]. Au nanorodes (NRs) was also used to increase the surface area for antibody immobilization, leading to the enhanced dielectric voltammetry detection of CRP [67]. Moreover, Lee's group synthesize gram-scale biocompatible cubelike microstructures of glucosamine-functionalized copper (GlcN-CuMC's) by the integration of injection pump and ultrasonochemistry [68]. GlcN-CuMC's exhibited excellent features such as more crystallinity, and electrochemical feasibility toward biomolecule detection. Thus, they deposited this GlcN-CuMC's on a conventional gold-PCB (Au-PCB) electrode for CRP detection (Figure 6). The fabricated Au-PCB/GlcN-CuMC's enhanced the electrochemical activity and exhibited a characteristic voltammetric response against anti-CRP/CRP interaction. The LOD for CRP by the current devised protocol was 0.37 ng/mL. Porous metal-organic frameworks (MOFs) have become increasingly popular in various applications due to their merits. Dong's group used ionic liquid (IL)-dispersed MOFs (Zr-tdc) derived from Zr(IV) and 2,5-thiophenedicarboxylate ligand (H_2tdc) to modify the carbon paste electrode (CPE) and immobilize anti-CRP [69]. They also prepared a novel ZnO/porous carbon matrix (ZnO/MPC) through thermolysis of a mixed-ligand MOF (Zn-BDC-TED) for electrochemical immunosensing CRP

in real samples [70]. In the past decades, magnetic beads (MBs) have found numerous applications in biological and chemical fields, because of its large surface area, good bio-compatibility and facility to separation with an extra magnetic field. Abdelghani's group functionalized gold electrode with MBs and antibodies for CRP detection [71]. Ibupoto's group employed ZnO nanotubes (NTs) to modify the gold coated glass substrates and physically adsorbe anti-CRP antibodies [72].

Table 1 Comparison of analytical performance of electrochemical methods for CRP with antibody as the receptor.

| Electrode substrate	Method	Linear range	LOD	Ref.
GE	EIS	0.5–50 nmol/L	176 pmol/L	[32]
GID	ECS	$25-2.5\times10^4$ pg/mL	25 pg/mL	[33]
Au-SPE	DPV	6.25–50 μg/mL	0.78 μg/mL	[35]
GE	DPV	1.15×10^{-5}–1.15 μg/mL	6×10^{-6} μg/mL	[36]
nanoporous silica/GE	EIS	1–1000 pg/mL	1 pg/mL	[37]
3DOM gold film	EIS	0.1–20 ng/mL	0.1 ng/mL	[38]
Au wire/polycarbonate	SWV	5–220 fg/mL	3 fg/mL	[39]
SAM(DTSP)/IDWμE	ECS	$0.01-1\times10^4$ ng/mL	0.025 ng/mL	[40]
SAM (3-CPTMS)/ITO	EIS	3.25–208 fg/mL	0.455 fg/mL	[42]
SAM (11-FcC and pentadecanethiol)/GE	ECS	0.5–10 nmol/L	0.2 nmol/L	[43]
SAM (11-FcC and PEG)/GE	ECS	$50-1\times10^5$ pmol/L	28 pmol/L	[44]
11-FcC/GO/CBMA/GE	ECS	$50-5\times10^4$ pmol/L	18.3 pmol/L	[45]
SAM (Fc-peptide)/GE	ECS	0.5–10 nmol/L	0.8 nmol/L	[46]
PATP/graphite electrode	DPV	$75-1.5\times10^5$ ng/mL	7.24 ng/mL	[47]
PANI-PA/SPE	ECS	0.25−2 μg/mL	0.5 μg/mL	[48]
Au(MPA)-PPy/ITO	EIS	$10-1\times10^4$ ng/mL	19.38 ng/mL	[49]
Pt(MPA)-NPs-PPy/ITO	EIS	$10-1\times10^4$ ng/mL	4.54 ng/mL	[50]
MoS_2–PANI–GNPs	DPV	0.2–80 ng/mL	0.04 ng/mL	[51]
PEI-Fc/GCE	DPV	$1-5\times10^4$ ng/mL	0.5 ng/mL	[53]
PAMAM/ITO	EIS	21–6148 fg/mL	0.34 fg/mL	[54]
PEG/GE	EIS	0.5–50 nmol/L	150 ± 10 pmol/L	[52]
NFCs/PEI-gold chips	QCM	1–100 μg/mL	none	[55]
MWCNTs/CF/GE	EIS	0.084–0.84 nmol/L	0.04 nmol/L	[56]
MWCNT–GMP/CoRb-SPCE	DPV	0.3–100 μg/mL	0.16 μg/mL	[57]
AuNPs/G/SPE	EIS	0.05–100 μg/mL	15 μg/mL	[58]
Pt NPs-graphene/SPE	EIS	0.01–10 μg/ml	8.4 ng/mL	[59]
rGO-NP/ITO	EIS	1–1000 ng/mL	0.06 ng/mL	[60]
GQD/GCE	EIS	0.5–70 nmol/L	0.176 nmol/L	[61]
VACNFs/NEA	EIS	0.05–5 μg/mL	0.011 μg/mL	[63]
NCD	EIS	12.5–1250 μg/mL	12.5 μg/mL	[65]
Au NPs/GE	Potential	5–25 μg/mL	none	[66]
AuNRs/nanogapped electrode	voltammetry	$0.01-1\times10^3$ pmol/L	0.01 pmol/L	[67]
Au-PCB/GlcN-CuMC's	CV	0.37–10 ng/mL	0.37 ng/mL	[68]
Zr-tdc/CPE	DPV	0.5–50 ng/mL 50–600 ng/mL	0.2 ng/mL	[69]
ZnO/MPC/CPE	DPV	0.01–1000 ng/mL	5.0 pg/mL	[70]
MBs/GE	EIS	0.1–1 pg/mL	0.1 pg/mL	[71]
ZnO NTs	Potential	1×10^{-5}–1 μg/mL	1×10^{-6} μg/mL	[72]
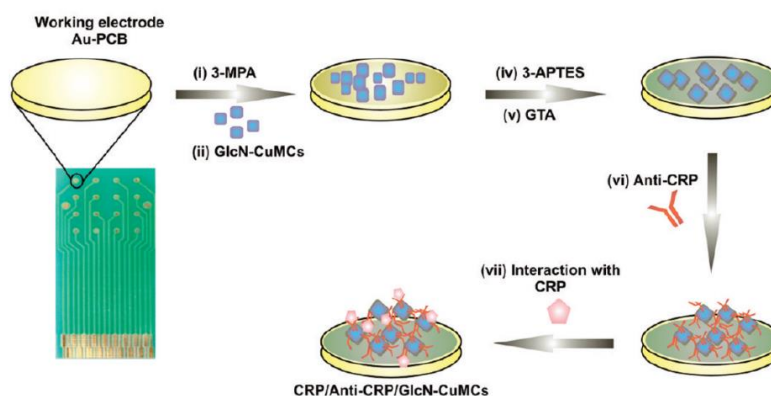
Figure 6. Illustration of the preparation of the Au-PCB/GlcN-CuMC's biosensor platform. Reprinted with permission from reference [68]. Copyright 2011 American Chemical Society.

2.2 Other receptors

Most of CRP bioassays reported in the literature are usually based on the formation of an Ab-Ag complex. However, the production of antibodies in monoclonal or polyclonal form in animal hosts is time-consuming and antibodies immobilized on surfaces commonly do not perform as well as in homogeneous state [73]. Thus, scientists have put intensively effort into exploring new biorecognition elements for the biosensor development (Table 2).

It has been well characterized that CRP can bind with many phosphate esters (such as phosphocholine (PC) and phosphoethanolamine) with a phosphoryl ester moiety ($-OPO_3H$) and a cationic amine group ($-NR^{3+}$) in the presence of calcium ions. Thus, PC derivates always are used as artificial CRP receptors to design CRP assays. Merritt's synthesized two crown ether-phosphate ester ionophores with high affinity for CRP (Crown-PEA and Crown-PC) [74]. The synthetic route and structures of two compounds were shown in Figure 7. Changes in proton nuclear magnetic resonance (H-NMR) spectra of Crown-PC before and after addition of CRP was investigated to determine the degree of CRP binding to the ionophore. As a result, they incorporated these two ionophores into poly (vinyl chloride) (PVC) membrane electrodes for simple and inexpensive K^+ and CRP detection. The binding of targets to the ionophore at the membrane/solution interface would reduce the mobility of the ionophore-cation complex in the membrane phase, resulting in the proportional change in membrane potential. The performance of Crown-PC-based biosensor is better than that of Crown-PEA, since Crown-PC possesses more efficient binders for CRP. Laiwattanapaisal's group developed a folding affinity paper-based electrochemical impedance device (PEID) comprising a PC-modified dual SPE for label-free EIS CRP detection [75]. Prasad's used two functional monomers mimicking PC to self-assemble into a CRP-imprinted polymer film on the surface of SPCEs via "grafting-to" approach [76]. Moreover, MWCNTs was introduced into the film to enhance the sensitivity of the biosensor. Miyahara's group synthesized a conducting polymer possessing a zwitterionic PC group for developing electrochemical biosensors for CRP biosensing [77]. As shown in Figure 8, poly(3,4-ethylenedioxythiophene (EDOT)) (PEDOT) bearing PC groups was electropolymerized onto a glassy carbon electrode via the randomly copolymerization of EDOT and its derivate bearing a PC group

(EDOTPC) with a dopant sodium perchlorate. The conductivities and CRP recognition capability of the biocompatible conducting copolymer films could be finely tuned by varying the content of EDOTPC. Accompanied with the specific interaction of CRP with PC in a Ca^{2+}-containing buffer solution, the altered redox reaction between the indicators $[Fe-(CN)_6^{3-}/Fe(CN)_6^{4-}]$ could be measured by DPV. Finally, this conducting polymer-based protein biosensor achieved a dynamic range of $10-160$ nM with a LOD of 37 nM. Luo's group applied this anti-fouling PC-immobilized PEDOT film to monitor the specific interaction of CRP with PC groups by QCM [78]. Besides, thiol-terminated poly(2-methacryloyloxyethyl phosphorylcholine) (PMPC-SH) was also self-assembled on an Au NPs-modified SPE with paper-based analytical devices (PADs) by Chailapakul's group for determining CRP [79].
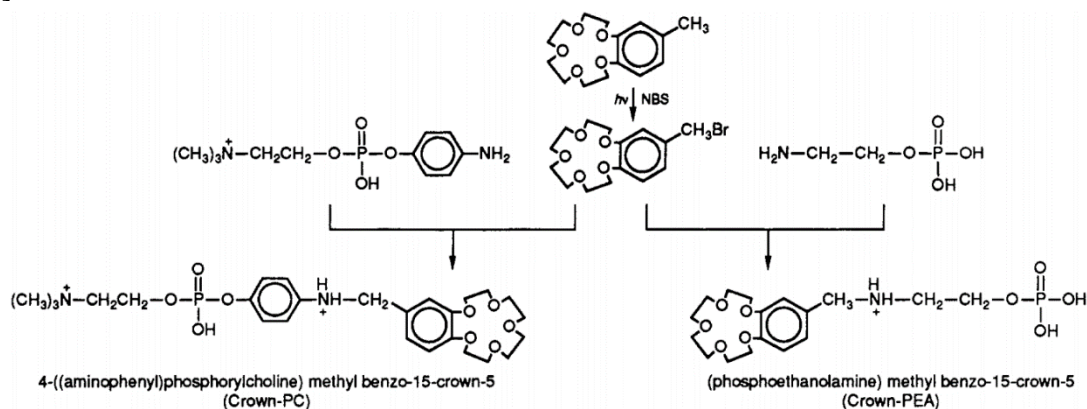

Figure 7. Preparation of Crown-PC and Crown-PEA. Reprinted with permission from reference [74]. Copyright 1989 American Chemical Society.
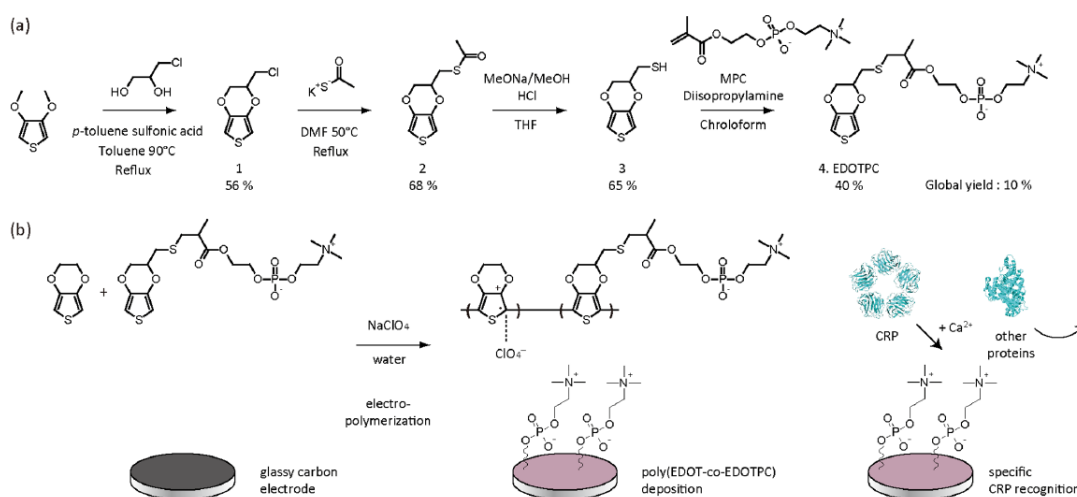

Figure 8. Schematic of the synthesis of EDOTPC and the functionalization of an electrode with conducting polymer for CRP biosensing. Reprinted with permission from reference [77]. Copyright 2015 American Chemical Society.

Aptamers with specific binding ability are single-stranded DNA or RNA oligonucleotides belonging to the group of so-called "functional nucleic acids", which are semi-synthetically produced through the SELEX technique (systematic evolution of ligands by exponential enrichment). Aptamers have been selected against a wide number of targets of interest, from low molecular weight inorganic

substrates to proteins and cells. Compared with antibodies, aptamers have several advantages such as highly chemical stability, high detection sensitivity and selectivity, the feasibility of adding functionality by chemical modification of sequences and can be synthesized in vitro for any given target. During an electrochemical experiment, redox indicator can interact with aptamer via electrostatic attraction/repulsion, π-π stacking with aromatic rings of nucleobases, and intercalation and binding to a minor groove. The formation of targets/aptamers complex would change the comfiguration and electronic properties of the biorecognition layers, resulting in the corresponding change of electrochemical signal. Jarczewska's group developed RNA and DNA aptamer-based electrochemical sensor for CRP detection, respectively, in which thiolated DNA aptamer was modifed on the surface of gold electrode and MB was used as the redox indicator [80, 81]. Synthetic RNA aptamers have also been immobilized onto the gold interdigitated (GID) capacitor arrays to develop capacitive biosensors for the detection of CRP by non-Faradaic impedance spectroscopy (NFIS) [82,83]. But, the high susceptibility of RNA aptamers to degradation by nucleases severely limit the application of RNA-based biosensors.

To overcome this shortcome, DNA analogue of the 44-nucleotide RNA aptamer was selected as alternative for conctructing a recognition layer for CRP capture. DNA aptamers not only possess higher stability than RNA probes, but also can be more efficiently and cheaply modify at their 5' or 3' ends with different functional groups. Davis's group reported an impedance-derived ECS assaying of CRP at a redox peptide supported aptamer interface (Figure 9) [84]. In this work, the simple electrochemically active peptide Fc-Glu-Ala-Ala-Cys was adsorbed on the gold electrode surface and further modified with the CRP DNA aptamer. The aptamer interface responds sensitively to CRP of 10−5000 pM as assessed at the E_{in} potential of 0.36 V. Wu's group developed a condutive nanowire-mesh biosensor for detection of serum CRP in melanoma by using both CRP DNA and RNA aptamer [85]. Even so, DNA/RNA aptamers still face several problems such as cation sensitivity and relatively weak biding strength to target.
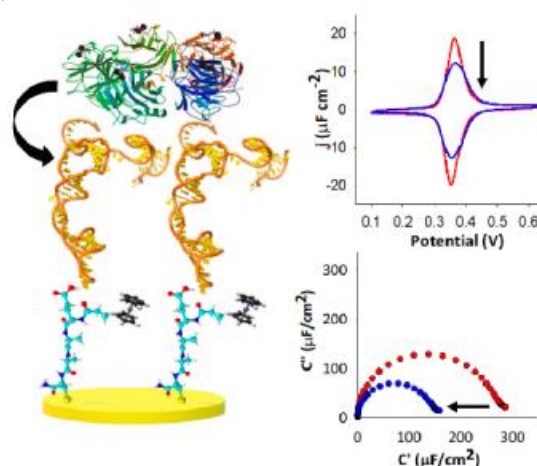

Figure 9. Representative schematic of the redox charging peptide-aptamer SAM and associated voltammetric response. Reprinted with permission from reference [84]. Copyright 2018 American Chemical Society.

Peptide aptamers, one class of engineered nonantibody probe molecules, are conformationally constrained within the structure of a constant scaffold protein. Affimers are peptide aptamers based on

the Stefin A scaffold, which have been used to replace antibodies in many detection platforms. Davis' group developed sensitive antibody-and-affimer based immunoassays for CRP and for the first time compared their performance using microarray experiments, SPR, and EIS (Figure 10) [86]. Disappointingly, the results showed that antibody interfaces outperform affimers interfaces in optical assays. But, in an EIS format, affimers-based interfaces showed the comparable performance, attributed to the relative sizes of two affimers molecules. Accordingly, a receptive surface derived from smaller affimer may extend only 3 nm away from the transducing surface. Moreover, as displayed in Figure 10, smaller affimers left a large gate for the redox probe mobility, associated with a low initial charge transfer resistance. Therefore, affimers-based interfaces are very sensitive to target binding.
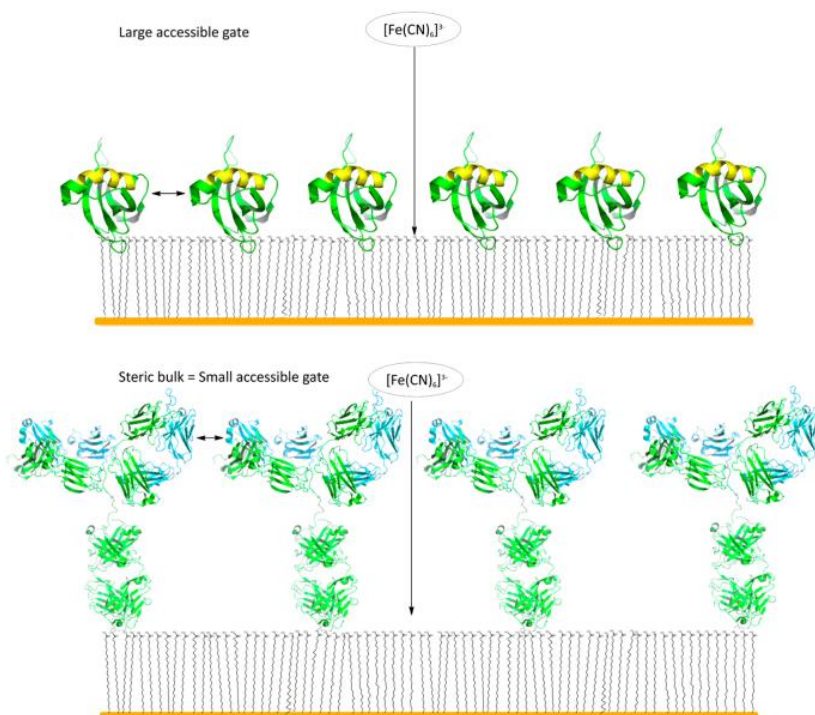

Figure 10. Schematic representation of the antibody (lower) and P7i22 Affimer (upper) interfaces on a PEGylated gold electrode (to relative scale). Reprinted with permission from reference [86]. Copyright 2012 American Chemical Society.

Table 2 Comparison of analytical performance of electrochemical methods for CRP using other molecules as capture probes.

Capture probes	Method	Electrode substrate	Linear range	LOD	Ref.
PC	EIS	PEID	0.005–500 g/mL	0.001 g/mL	[75]
	DPV	MWCNTs/MIP- SPCE	0.18–8.51 g/mL	0.04 g/mL	[76]
	DPV	EDOT/GCE	0.5–50 nmol/L	37 nmol/L	[77]
	DPV	PMPC-SH/SPE	$5–5 \times 10^3$ ng/mL	1.6 ng/mL	[79]
RNA aptamer	ECS	GID	100−500 pg/mL	none	[82]
	ECS	CNT-GID	1–8 mol/L	none	[83]
	SWV	GE	1–100 pmol/L	none	[80]
DNA aptamer	SWV	GE	1–100 pmol/L	none	[81]
	ECS	Fc-peptide/GE	1–5000 pmol/L	7.2 ± 2.4 pmol/L	[84]
DNA/RNA aptamer	EIS	CuPT-PPy/NIPAAm-AM	none	7.85×10^{-19} mol/L	[85]

3. SANDWHICH-TYPE BIOSENSORS

Due to the lack of typical electrochemical signal of antigens and antibodies, it is important for sandwich-type biosensors to label detection antibody with electroactive or electro-catalytic molecules, biomolecules or NMs (Table 3). Organic molecules with redox properties are usually used as electrochemical labels because of their stable redox activity and small sizes which could minimize the interference with the biomolecular interaction. For example, anthraquinone (AQ) has been introduced to electrochemical bioassays for biomolecules. Chailapakul's group used AQ to label Ab_2 and measured CRP concentrations by DPV in a sandwich-type assay format [87]. Unfortunately, too low ratio (1:1) of signal molecules to immune-reaction event drastically damages the sensitivity of this type biosensors.

Electrochemical biosensors based on enzymatic reactions, such as horseradish peroxidise (HRP), glucose oxidase (GOx), and alkaline phosphatase (ALP), provide high, steady, and reproducible signal amplification. Centi's group developed an electrochemical aptamer-based sandwich magnetoimmunosensor with ALP as the enzymatic label involving MBs and SPCEs [88]. After the sandwich assay and magnetic separation, ALP captured on the surface of SPCEs hydrolyzed α-naphthyl-phosphate into α-naphthol, which could be detected by DPV. HRP can also be used as the label to prepare magnetoimmunosensor for CRP quantification with TMB as electron transfer mediator and H_2O_2 as the enzyme substrate [89,90]. For example, Escarpa's group constructed a dual magnetoimmunosensor for simultaneous procalcitonin (PCT) and CRP detection in a small volume of diagnosed clinical samples (Figure. 11) [91]. HRP enzyme conjugated with anti-CRP is used as enzyme label for both immunosensors. The results showed that at fixed measured time (60 s), cross-talk by diffusion of the enzymatic reaction product between both working electrodes was negligible. The LODs were obtained to be 0.09 ng/mL PCT and 0.008 μg/mL CRP, respectively. Cho's group further designed a flow-enhanced HRP-catalyzed electrochemical CRP immunosensors on an integrated centrifugal microfluidic platform [92]. Gan's group developed a piezoelectric immunosensor based on $Fe_3O_4@SiO_2$ magnetic capture nanoprobes and HRP-antibody co-carried Au NPs as signal tags [93]. After the magnetic separation and immobilization, vast HRP catalyzed the oxidation of 3-amino-9-ethylcarbazole (AEC) by H_2O_2 to yield more AEC's insoluble oxidation product on piezoelectric crystal surface. Aiming enhancing the sensitivity of immunoassays, Pyun's group immobilized E. coli cell with autodisplayed Z-domains for the orientation control of Ab_1 and the HRP-catalyzed reaction of TMB was used to report the immune-reaction event [94]. Protein A was used to ensure the oriented immobilization of anti-CRP antibodies by Rishpon's group on the CNTs-modified SPEs [95]. Lin's group reported an electrochemical Proton-ELISA (H-ELISA) for CRP on a dual-gated ion-sensitive field effect transistor (ISFET) array, which detect protons in immunoassay detection medium, generated by GOx coupled with Fenton's reagent in the presence of glucose [96]. However, these enzymatic biosensors often suffer from severe limitations including instability, high price and poor reusability, which largely block their practical applications.

Since the discovery of iron oxide nanoparticles (NPs) with enzyme mimic properties, increasing numbers of NMs have been reported possessing enzyme-mimic ability to meet imperious demands for signal amplification, which could be utilized in the development of novel and sensitive

biosensors. For example, Yang's group have used hollow silver platinum ((hAg–Pt) NPs and Co_3O_4 NPs as nano-mimetic enzymes for preparing CRP electrochemical immunosensors [97,98].
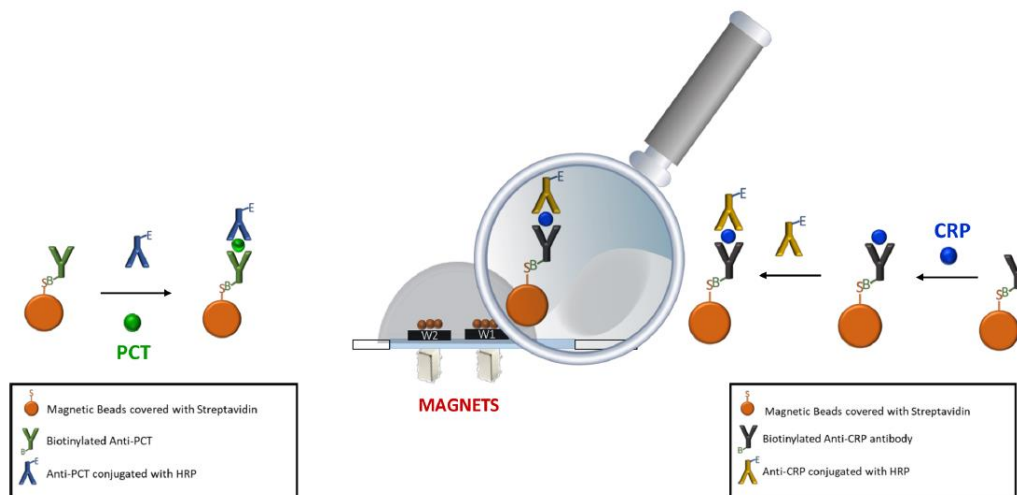

Figure 11. Detailed schematic representation of the electrochemical magnetoimmunoassay strategy for the simultaneous detection of PCT and CRP. Reprinted with permission from reference [91]. Copyright 2019 American Chemical Society.
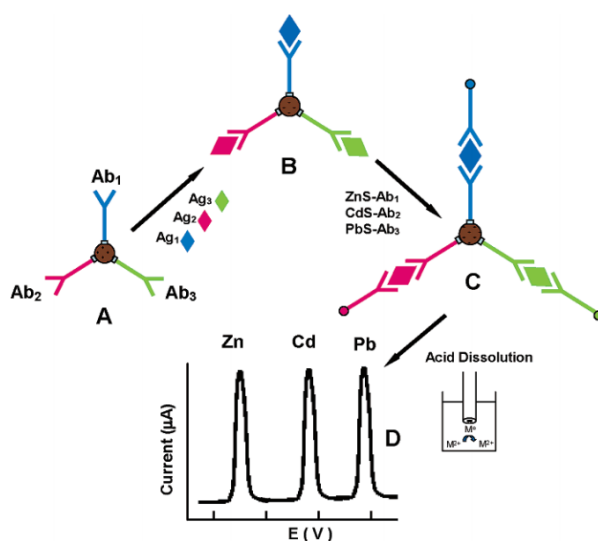

Figure 12. Schematic illustration of multiprotein electrical detection protocol based on different QDs as tracers. Reprinted with permission from reference [99]. Copyright 2004 American Chemical Society.

Besides excellent fluorescence properties, semiconductor quantum dots (QDs) have been widely utilized as electrochemical tracers to develop biosensors for detection of targets because of ease of preparation and functionalization and large amounts of electroactive metal elements in QDs. For instance, Wang's group developed an electrochemical immunobiosensor for the simultaneous measurements of proteins, including CRP, by using different QDs tracers (Figure 12) [99]. In a binding event, Ab-labeled QDs was captured by Ab-labeled MBs. Then, resulting sandwich-like immune-complexes were dissolved by HNO_3 solution into corresponding metal ions, which was then transferred into supporting electrolyte solution and detected by square-wave anodic stripping

voltammetry (SWASV). Zhu's group also employed CdTe and ZnSe QDs as tracers for simultaneous detection of cardiac troponin I (cTnI) and CRP by SWASV integrated with a poly(dimethylsiloxane)-Au NPs microfluidic chip [100]. Kokkinos' group proposed an QDs-based electrochemical immunosensor for the voltammetric determination of CRP in human serum using bismuth citrate modified graphite screen-printed electrodes (SPEs) [101]. However, electrochemical biosensors with QDs as signal tracers generally suffer from prominent disadvantages of too long soaking time and tedious procedures.

Generally, NMs are chiefly employed as supporting materials for loading enzymes or signal molecules. However, it is beneficial that NMs can directly generate electrochemical signals, which will simplify the experiment procedures and accelerate the signal transduction process. Metal−organic frameworks (MOFs), consisting of metal ions or clusters linked by organic bridging ligands, have aroused extensive interest because of the excellent properties such as high surface areas, tunable physicochemical properties, and high density of metal sites. By elaborately choosing metal ions or organic linkers, MOFs can act as not only nanozymes or electrocatalysts for signal amplification but also signal probes. For example, Yang's group for the first time reported that MOFs, HKUST-1 themselves could be used as signal probe for ultrasensitively sensing CRP (Figure 13) [102]. They used Pt NPs modified covalent organic frameworks (COFs) with high surface area and electronic conductivity to modify the GC electrode and decorated HKUST-1 with Au NPs for Ab_2 conjugation. During the electrochemical measurement, large amounts of Cu^{2+} ions in HKUST-1 can directly produce typical electrochemical reduction signal at −0.02 V in buffer solutions, accompanying with the collapse of the topological structure of MOFs. Under the optimal experimental conditions, this novel method achieved a linear dynamic ranging from 1 to 400 ng/mL and a LOD of 0.2 ng/mL. More importantly, the proposed sensing strategy is simple and low-cost without the need of harsh acid dissolution steps. Owing to the suitable electrochemical oxidation potential, silver and copper NPs can also be directly used as signal probes [103-105]. Zhang's group constructed an electrochemical immunosensor for CRP detection, in which Cu NPs was in situ generated in the product long DNA concatemers of hybridization chain reaction [106]. After loading with electroactive metal ions (such as Zn^{2+} Cu^{2+} and Pb^{2+}), reduced graphene oxide-tetraethylene pentaamine, Au NPs-functionalized silica microspheres and polydopamine nanospheres were used as signal probes to detect CRP [107-109].
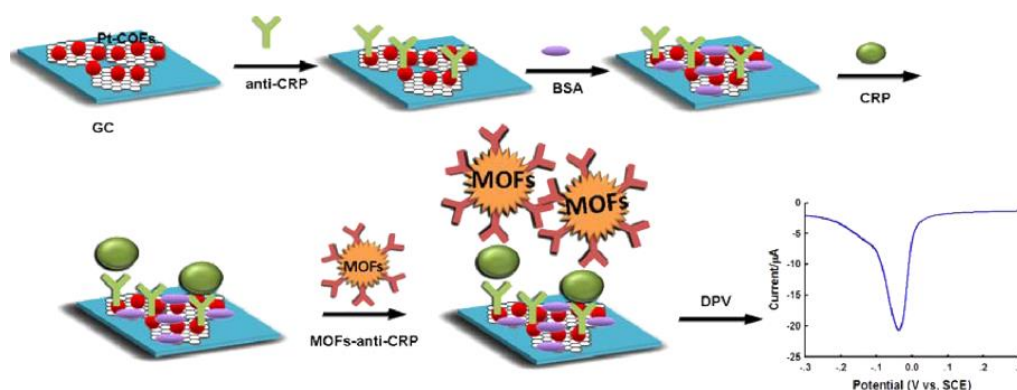

Figure 13. Schematic illustration of the electrochemical immunosensor for CRP based on MOF HKUST-1. Reprinted with permission from reference [102]. Copyright 2016 American Chemical Society.

In the past few years, redox molybdophosphate precipitate formed by the reaction of phosphate groups with molybdate, which could generate a stable electrochemical current, have been widely introduced into the development of various electrochemical biosensors [110,111]. Li's group used polydopamine-coated $Cu_3(PO_4)_2$ nanospheres (NSs) as signal probes for CRP detection because abundant phosphate groups in NSs could react with adscititious molybdate ions to form redox-active molybdophosphate precipitate on the electrodes [112]. Titanium phosphate NSs was also used to develop CRP immunosensor based on the same detection strategy [113]. Recently, they successfully prepared BSA-antibodies-copper phosphate hybrid nanoflowers (BSA-Ab$_2$-Cu$_3$(PO$_4$)$_2$) as signal probes, which greatly increased the sensitivity of the fabricated CRP immunosensors [114].

Table 3 Comparison of analytical performance of sandwich-type electrochemical methods for CRP detection.

Labels	Method	Electrode substrate	Linear range	LOD	Ref.
AQ	DPV	AuNPs/SPGE	0.01–150 µg/mL	1.5 ng/mL	[87]
ALP	DPV	CE/magnet	0.1–50 µg/mL	54 ng/mL	[88]
HRP	Amperometry	MBs/Au-SPE	0.07–1000 ng/mL	0.021 ng/mL	[89]
HRP	Amperometry	dSPCEs	2–100 ng/mL	0.47 ng/mL	[115]
HRP	Amperometry	dSPCEs	0.01–5.0 µg/mL	0.008 µg/mL	[91]
HRP	Amperometry	GE	none	4.9 pg/mL	[92]
Au NPs-HRP	QCM	QCM chip	0.001–100 ng/mL	0.3 pg/mL	[93]
HRP	Amperometry	CNTs/SPE	0.5–500 ng/mL	0.5 ng/mL	[95]
Hollow Ag–Pt	chronoamperometry	GO/CHIT/GCE	0.5–140 ng/mL	0.17 ng/mL	[97]
Co_3O_4 NPs	Amperometry	Au NPs-COFs/GCE	0.05–80 ng/mL	0.017 ng/mL	[98]
QDs	SWV	PDMS-Au NPs	0.5–200 ng/mL	0.22 ng/mL	[100]
PbS QDs	ASV	Bi-SPE	0.2–100 ng/mL	0.05 ng/mL	[101]
Au-MOFs	DPV	Pt-COFs/GCE	1–400 ng/mL	0.2 ng/mL	[102]
Cu NPs	DPV	Au NPs/GCE	$1–1\times10^8$ fg/mL	0.33 fg/mL	[106]
rGO-TEPA-Pb^{2+}	DPV	Au@BSA/GCE	0.05–100 ng/mL	0.0167 ng/mL	[107]
Si MSs-AuNPs-Zn^{2+}	SWV	Au NPs/GCE	0.005–125 ng/mL	0.0017 ng/mL	[108]
Metal-PDA NSs	SWV	PDA NS/GCE	$0.5–1\times10^3$ pg/mL	0.17 ng/mL	[109]
$Cu_3(PO_4)_2$ NSs	SWV	PDA/rGO/GCE	$0.5–1\times10^3$ pg/mL	0.13 pg/mL	[112]
BSA-Cu$_3$(PO$_4$)$_2$ NFs	SWV	PDA NS/GCE	$5–1\times10^3$ pg/mL	1.26 pg/mL	[114]
MB	SWV	NH$_2$-Ni-MOF/GE	$0.1–1\times10^5$ pg/mL	0.029 pg/mL	[116]

4. CONCLUSION

Significant achievements in the field of electrochemical biosensors make single and multiple biomarker assays highly promising in improving the reliability and speed of diagnosis and treatment monitoring. This review shows that the biosensors offer unique opportunities and simple protocols for the determination of CPR at different levels. Although the proposed biosensors show great potential, the requirements for direct determination of CPR in protein rich samples or at extreme pH values is still faced with important challenges.

References

1.   A. May and T. J. Wang, *Expert Rev. Mol. Diagn.*, 7 (2007) 793.
2.   W. L. Roberts, Cdc and Aha, *Circulation*, 110 (2004) e572.
3.   O. Deegan, K. Walshe, K. Kavanagh and S. Doyle, *Anal. Biochem.*, 312 (2003) 175.
4.   M. Kjelgaard-Hansen, S. Martinez-Subiela, H. H. Petersen, A. L. Jensen and J. J. Ceron, *Vet. J.*, 173 (2007) 571.
5.   N. E. Thomas and W. T. Coakley, *Ultrasound Med. Biol.*, 22 (1996) 1277.
6.   T. L. Wu, I. C. Tsai, P. Y. Chang, K. C. Tsao, C. F. Sun, L. L. Wu and J. T. Wu, *Clin. Chim. Acta*, 376 (2007) 72.
7.   S. K. Vashist, G. Czilwik, T. van Oordt, F. von Stetten, R. Zengerle, E. Marion Schneider and J. H. Luong, *Anal. Biochem.*, 456 (2014) 32.
8.   S. K. Vashist, T. van Oordt, E. M. Schneider, R. Zengerle, F. von Stetten and J. H. Luong, *Biosens. Bioelectron.*, 67 (2015) 248.
9.   N. Xia, D. Deng, X. Mu, A. Liu, J. Xie, D. Zhou, P. Yang, Y. Xing and L. Liu, *Sens. Actuat. B: Chem.*, 306 (2020) 127571.
10. M. H. Meyer, M. Hartmann and M. Keusgen, *Biosens. Bioelectron.*, 21 (2006) 1987.
11. W. P. Hu, H. Y. Hsu, A. Chiou, K. Y. Tseng, H. Y. Lin, G. L. Chang and S. J. Chen, *Biosens. Bioelectron.*, 21 (2006) 1631.
12. J. Y. Byun, Y. B. Shin, D. M. Kim and M. G. Kim, *Analyst*, 138 (2013) 1538.
13. P. Wang, B. Jin, Y. Xing, Z. Cheng, Y. Ge, H. Zhang, B. Hu, H. Mao, Q. Jin and J. Zhao, *J. Nanosci. Nanotechnol.*, 14 (2014) 5662.
14. S. K. Vashist, E. Marion Schneider, R. Zengerle, F. von Stetten and J. H. Luong, *Biosens. Bioelectron.*, 66 (2015) 169.
15. H. Kim, E. Kim, E. Choi, C. S. Baek, B. Song, C.-H. Cho and S. W. Jeong, *RSC Adv.*, 5 (2015) 34720.
16. S. Wang, J. Luo, Y. He, Y. Chai, R. Yuan and X. Yang, *ACS Appl. Mater. Interfaces*, 10 (2018) 33707.
17. J. Pultar, U. Sauer, P. Domnanich and C. Preininger, *Biosens. Bioelectron.*, 24 (2009) 1456.
18. M. S. Islam, H. Yu, H. G. Lee and S. H. Kang, *Biosens. Bioelectron.*, 26 (2010) 1028.
19. E. D. Bernard, K. C. Nguyen, M. C. DeRosa, A. F. Tayabali and R. Aranda-Rodriguez, *Anal. Biochem.*, 472 (2015) 67.
20. M. S. Islam and S. H. Kang, *Talanta*, 84 (2011) 752.
21. W. Zhan and A. J. Bard, *Anal. Chem.*, 79 (2007) 459.
22. T. Ylinen-Hinkka, A. J. Niskanen, S. Franssila and S. Kulmala, *Anal. Chim. Acta*, 702 (2011) 45.
23. M. J. Li, H. J. Wang, R. Yuan and Y. Q. Chai, *Chem. Commun.*, 55 (2019) 10772.
24. X. Zhang, K. N. Chi, D. L. Li, Y. Deng, Y. C. Ma, Q. Q. Xu, R. Hu and Y. H. Yang, *Biosens. Bioelectron.*, 129 (2019) 64.
25. C. Chen, Y. Feng, X. Xia, M. La and B. Zhou, *Int. J. Electrochem. Sci.*, 14 (2019) 5174.
26. M. La, C. Chen, X. Xia, J. Zhang and B. Zhou, *Int. J. Electrochem. Sci.*, 14 (2019) 5547.
27. D. Deng, L. Liu, Y. Bu, X. Liu, X. Wang and B. Zhang, *Sens. Actuat. B: Chem.*, 269 (2018) 189.
28. N. Xia, Z. Chen, Y. Liu, H. Ren and L. Liu, *Sens. Actuat. B: Chem.*, 243 (2017) 784.
29. N. Xia, D. Deng, S. Yang, Y. Hao, L. Wang, Y. X Liu, C. An, Q. Han and L. Liu, *Sens. Actuat. B: Chem.*, 291 (2019) 113.
30. N. Xia, X. Wang, J. Yu, Y. Wu, S. Cheng, Y. Xing and L. Liu, *Sens. Actuat. B: Chem.*, 239 (2017) 834.
31. X. Zeng, Z. Shen and R. Mernaugh, *Anal. Bioanal. Chem.*, 402 (2012) 3027.
32. T. Bryan, X. Luo, P. R. Bueno and J. J. Davis, *Biosens. Bioelectron.*, 39 (2013) 94.

33.   A. Qureshi, J. H. Niazi, S. Kallempudi and Y. Gurbuz, *Biosens. Bioelectron.*, 25 (2010) 2318.
34.   I. Hafaiedh, H. Chammem, A. Abdelghani, E. Ait, L. Feldman, O. Meilhac and L. Mora, *Talanta*, 116 (2013) 84.
35.   L. O. Resende, A. C. H. de Castro, A. O. Andrade, J. M. Madurro and A. G. Brito-Madurro, *J. Solid State Electrochem.*, 22 (2017) 1365.
36.   H. Hennessey, N. Afara, S. Omanovic and A. L. Padjen, *Anal. Chim. Acta*, 643 (2009) 45.
37.   K.-C. Lin, V. Kunduru, M. Bothara, K. Rege, S. Prasad and B. L. Ramakrishna, *Biosens. Bioelectron.*, 25 (2010) 2336.
38.   X. Chen, Y. Wang, J. Zhou, W. Yan, X. Li and J.-J. Zhu, *Anal. Chem.*, 80 (2008) 2133.
39.   A. T. E. Vilian, W. Kim, B. Park, S. Y. Oh, T. Kim, Y. S. Huh, C. K. Hwangbo and Y. K. Han, *Biosens. Bioelectron.*, 142 (2019) 111549.
40.   S. R. Chinnadayyala, J. Park, Y. H. Kim, S. H. Choi, S.-M. Lee, W. W. Cho, G.-Y. Lee, J.-C. Pyun and S. Cho, *Sensors*, 19 (2019)
41.   J.-Y. Park, Y.-S. Lee, B. H. Kim and S.-M. Park, *Anal. Chem.*, 80 (2008) 4986.
42.   M. N. Sonuc Karaboga and M. K. Sezginturk, *J. Pharm. Biomed. Anal.*, 154 (2018) 227.
43.   F. C. Fernandes, M. S. Goes, J. J. Davis and P. R. Bueno, *Biosens. Bioelectron.*, 50 (2013) 437.
44.   J. Lehr, F. C. Bedatty Fernandes, P. R. Bueno and J. J. Davis, *Anal. Chem.*, 86 (2014) 2559.
45.   F. C. B. Fernandes, J. R. Andrade and P. R. Bueno, *Sens. Actuat. B: Chem.*, 291 (2019) 493.
46.   A. Santos, J. P. Piccoli, N. A. Santos-Filho, E. M. Cilli and P. R. Bueno, *Biosens. Bioelectron.*, 68 (2015) 281.
47.   A. J. G. Lemos, R. P. A. Balvedi, V. R. Rodovalho, L. O. Resende, A. C. H. Castro, S. Cuadros-Orellana, J. M. Madurro and A. G. Brito-Madurro, *Microchem. J.*, 133 (2017) 572.
48.   A. Baradoke, R. Hein, X. Li and J. J. Davis, *Anal. Chem.*, 92 (2020) 3508.
49.   S. K. Mishra, V. Sharma, D. Kumar and Rajesh, *Appl. Biochem. Biotech.*, 174 (2014) 984.
50.   S. K. Mishra, A. K. Srivastava, D. Kumar, A. Mulchandani and Rajesh, *Polymer*, 55 (2014) 4003.
51.   X. Zhang, R. Hu, K. Zhang, R. Bai, D. Li and Y. Yang, *Anal. Methods*, 8 (2016) 6202.
52.   X. Luo, Q. Xu, T. James and J. J. Davis, *Anal. Chem.*, 86 (2014) 5553.
53.   A. Kowalczyk, J. P. Sek, A. Kasprzak, M. Poplawska, I. P. Grudzinski and A. M. Nowicka, *Biosens. Bioelectron.*, 117 (2018) 232.
54.   M. N. Sonuc Karaboga and M. K. Sezginturk, *Talanta*, 186 (2018) 162.
55.   Y. Zhang and O. J. Rojas, *Biomacromolecules*, 18 (2017) 526.
56.   Y. Jang, H. Kim, S. Y. Yang, J. Jung and J. Oh, *Nanoscale*, (2020) 1.
57.   S. L. Zeng, H. K. Zhou, N. Gan and Y. T. Cao, *Appl. Mech. Mater.*, 80-81 (2011) 452.
58.   S. Boonkaew, S. Chaiyo, S. Jampasa, S. Rengpipat, W. Siangproh and O. Chailapakul, *Microchim. Acta*, 186 (2019) 153.
59.   S. Singal, A. M. Biradar, A. Mulchandani and Rajesh, *Appl. Biochem. Biotech.*, 174 (2014) 971.
60.   A. K. Yagati, J. C. Pyun, J. Min and S. Cho, *Bioelectrochemistry*, 107 (2016) 37.
61.   X. Bing and G. Wang, *Int. J. Electrochem. Sci.*, 12 (2017) 6304.
62.   A. Periyakaruppan, R. P. Gandhiraman, M. Meyyappan and J. E. Koehne, *Anal. Chem.*, 85 (2013) 3858.
63.   R. K. Gupta, A. Periyakaruppan, M. Meyyappan and J. E. Koehne, *Biosens. Bioelectron.*, 59 (2014) 112.
64.   R. K. Gupta, R. Pandya, T. Sieffert, M. Meyyappan and J. E. Koehne, *J. Electroanal. Chem.*, 773 (2016) 53.
65.   V. Vermeeren, L. Grieten, N. Vanden Bon, N. Bijnens, S. Wenmackers, S. D. Janssens, K. Haenen, P. Wagner and L. Michiels, *Sens. Actuat. B: Chem.*, 157 (2011) 130.
66.   J. J. Zhu, J. Z. Xu, J. T. He, Y. J. Wang, Q. Miao and H. Y. Chen, *Anal. Lett.*, 36 (2003) 1547.

67. I. Letchumanan, M. K. M. Arshad, S. R. Balakrishnan and S. C. B. Gopinath, *Biosens. Bioelectron.*, 130 (2019) 40.
68. M. Veerapandian, R. Subbiah, G.-S. Lim, S.-H. Park, K. Yun and M.-H. Lee, *Langmuir*, 27 (2011) 8934.
69. S. Dong, H. Cui, D. Zhang and M. Tong, *J. Electrochem. Soc.*, 166 (2019) B193.
70. S. Dong, D. Zhang, H. Cui and T. Huang, *Sens. Actuat. B: Chem.*, 284 (2019) 354.
71. H. Chammem, I. Hafaid, M. Ardhaoui, L. Mora, O. Meilhac and A. Abdelghani, *Int. J. Nanotech.*, 12 (2015) 552.
72. Z. H. Ibupoto, N. Jamal, K. Khun and M. Willander, *Sens. Actuat. B: Chem.*, 166 (2012) 809.
73. J. R. Collett, E. J. Cho and A. D. Ellington, *Methods*, 37 (2005) 4.
74. C. M. Merritt and J. W. Winkelman, *Anal. Chem.*, 61 (1989) 2362.
75. Y. Boonyasit, O. Chailapakul and W. Laiwattanapaisal, *Biosens. Bioelectron.*, 130 (2019) 389.
76. D. Kumar and B. B. Prasad, *Sens. Actuat. B: Chem.*, 171 (2012) 1141.
77. T. Goda, M. Toya, A. Matsumoto and Y. Miyahara, *ACS Appl. Mater. Interfaces*, 7 (2015) 27440.
78. J.-G. Wu, S.-C. Wei, Y. Chen, J.-H. Chen and S.-C. Luo, *Langmuir*, 34 (2018) 943.
79. C. Pinyorospathum, S. Chaiyo, P. Sae-Ung, V. P. Hoven, P. Damsongsang, W. Siangproh and O. Chailapakul, *Microchim. Acta*, 186 (2019) 472.
80. M. Jarczewska, R. Ziółkowski, Ł. Górski and E. Malinowska, *Electroanalysis*, 30 (2018) 658.
81. M. Jarczewska, J. Rebis, L. Gorski and E. Malinowska, *Talanta*, 189 (2018) 45.
82. A. Qureshi, Y. Gurbuz, S. Kallempudi and J. H. Niazi, *Phy. Chem. Chem. Phy.*, 12 (2010) 9176.
83. A. Qureshi, I. Roci, Y. Gurbuz and J. H. Niazi, *Biosens. Bioelectron.*, 34 (2012) 165.
84. J. Piccoli, R. Hein, A. H. El-Sagheer, T. Brown, E. M. Cilli, P. R. Bueno and J. J. Davis, *Anal. Chem.*, 90 (2018) 3005.
85. Z.-T. Lin, Y. Li, J. Gu, H. Wang, Z. Zhu, X. Hong, Z. Zhang, Q. Lu, J. Qiu, X. Wang, J. Bao and T. Wu, *Adv. Funct. Mater.*, 28 (2018) 1802482.
86. A. Johnson, Q. Song, P. K. Ferrigno, P. R. Bueno and J. J. Davis, *Anal. Chem.*, 84 (2012) 6553.
87. S. Jampasa, W. Siangproh, R. Laocharoensuk, T. Vilaivan and O. Chailapakul, *Talanta*, 183 (2018) 311.
88. S. Centi, L. B. Sanmartin, S. Tombelli, I. Palchetti and M. Mascini, *Electroanalysis*, 21 (2009) 1309.
89. B. Esteban-Fernandez de Avila, V. Escamilla-Gomez, S. Campuzano, M. Pedrero, J. P. Salvador, M. P. Marco and J. M. Pingarron, *Sens. Actuat. B: Chem.*, 188 (2013) 212.
90. B. E.-F. n. de Ávila, V. Escamilla-Gómez, V. Lanzone, S. Campuzano, M.-A. Pedrero, D. Compagnone and J. M. Pingarrón, *Electroanalysis*, 26 (2014) 254.
91. A. Molinero-Fernandez, M. Moreno-Guzman, L. Arruza, M. A. Lopez and A. Escarpa, *ACS Sens.*, 4 (2019) 2117.
92. T.-H. Kim, K. Abi-Samra, V. Sunkara, D.-K. Park, M. Amasia, N. Kim, J. Kim, H. Kim, M. Madou and Y.-K. Cho, *Lab. Chip*, 13 (2013) 3747.
93. J. Zhou, N. Gan, T. Li, H. Zhou, X. Li, Y. Cao, L. Wang, W. Sang and F. Hu, *Sens. Actuat. B: Chem.*, 178 (2013) 494.
94. J.-K. Lee, Y. Gu, M. Park, J. Jose, M.-J. Kang and J.-C. Pyun, *Sens. Actuat. B: Chem.*, 175 (2012) 46.
95. M. Buch and J. Rishpon, *Electroanalysis*, 20 (2008) 2592.
96. D. S. Juang, C. H. Lin, Y. R. Huo, C. Y. Tang, C. R. Cheng, H. S. Wu, S. F. Huang, A. Kalnitsky and C. C. Lin, *Biosens. Bioelectron.*, 117 (2018) 175.
97. K. Dai, L. Zheng, N. Xu, Z. Yang, T. Guo, R. Hu and Y. Yang, *J. Nanosci. Nanotech.*, 17 (2017) 115.

98. Y. Ma, M. Lu, Y. Deng, R. Bai, X. Zhang, D. Li, K. Zhang, R. Hu and Y. Yang, *J. Biomed. Nanotech.*, 14 (2018) 1169.
99. G. D. Liu, J. Wang, J. Kim, M. R. Jan and G. E. Collins, *Anal. Chem.*, 76 (2004) 7126.
100. F. Zhou, M. Lu, W. Wang, Z.-P. Bian, J.-R. Zhang and J.-J. Zhu, *Clin. Chem.*, 56 (2010) 1701.
101. C. Kokkinos, M. Prodromidis, A. Economou, P. Petrou and S. Kakabakos, *Anal. Chim. Acta*, 886 (2015) 29.
102. T. Z. Liu, R. Hu, X. Zhang, K. L. Zhang, Y. Liu, X. B. Zhang, R. Y. Bai, D. Li and Y. H. Yang, *Anal. Chem.*, 88 (2016) 12516.
103. N. Xia, C. Cheng, L. Liu, P. Peng, C. Liu and J. Chen, *Microchim. Acta*, 184 (2017) 4393.
104. N. Xia, L. Liu, Y. Chang, Y. Hao and X. Wang, *Electrochem. Commun.*, 74 (2017) 28.
105. N. Xia, X. Wang, B. Zhou, Y. Wu, W. Mao and L. Liu, *ACS Appl. Mater. Interfaces*, 8 (2016) 19303.
106. J. Zhang, W. Zhang, J. Guo, J. Wang and Y. Zhang, *Anal. Biochem.*, 539 (2017) 1.
107. G. Yuan, C. Yu, C. Xia, L. Gao, W. Xu, W. Li and J. He, *Biosens. Bioelectron.*, 72 (2015) 237.
108. J. Wang, J. Guo, J. Zhang, W. Zhang and Y. Zhang, *Biosens. Bioelectron.*, 95 (2017) 100.
109. H. Li, W. Du, L. Jiao, L. Chen, B. Ran, M. Dong and Z. Qian, *J. Biomed. Nanotech.*, 13 (2017) 1235.
110. C. Shen, K. Zeng, J. Luo, X. Li, M. Yang and A. Rasooly, *Anal. Chem.*, 89 (2017) 10264.
111. L. Hu, S. Hu, L. Guo, C. Shen, M. Yang and A. Rasooly, *Anal. Chem.*, 89 (2017) 2547.
112. X. Tan, L. Zhang, X. Deng, L. Miao, H. Li and G. Zheng, *New J. Chem.*, 41 (2017) 11867.
113. X. Tan, L. Zhang, H. Li, S. Liu, L. Miao, H. Li and G. Zheng, *J. Biomed. Nanotech.*, 13 (2017) 973.
114. Q. Tang, L. Zhang, X. Tan, L. Jiao, Q. Wei and H. Li, *Biosens. Bioelectron.*, 133 (2019) 94.
115. B. E.-F. de Ávila, V. Escamilla-Gómez, V. Lanzone, S. Campuzano, M. Pedrero, D. Compagnone and J. M. Pingarrón, *Electroanalysis*, 26 (2014) 254.
116. Z. Wang, P. Dong, Z. Sun, C. Sun, H. Bu, J. Han, S. Chen and G. Xie, *J. Mater.Chem. B*, 6 (2018) 2426.